

JUNE 2023
VOLUME 39, ISSUE 6

TAKE A LOOK INSIDE
Industry Briefs
—see page 9

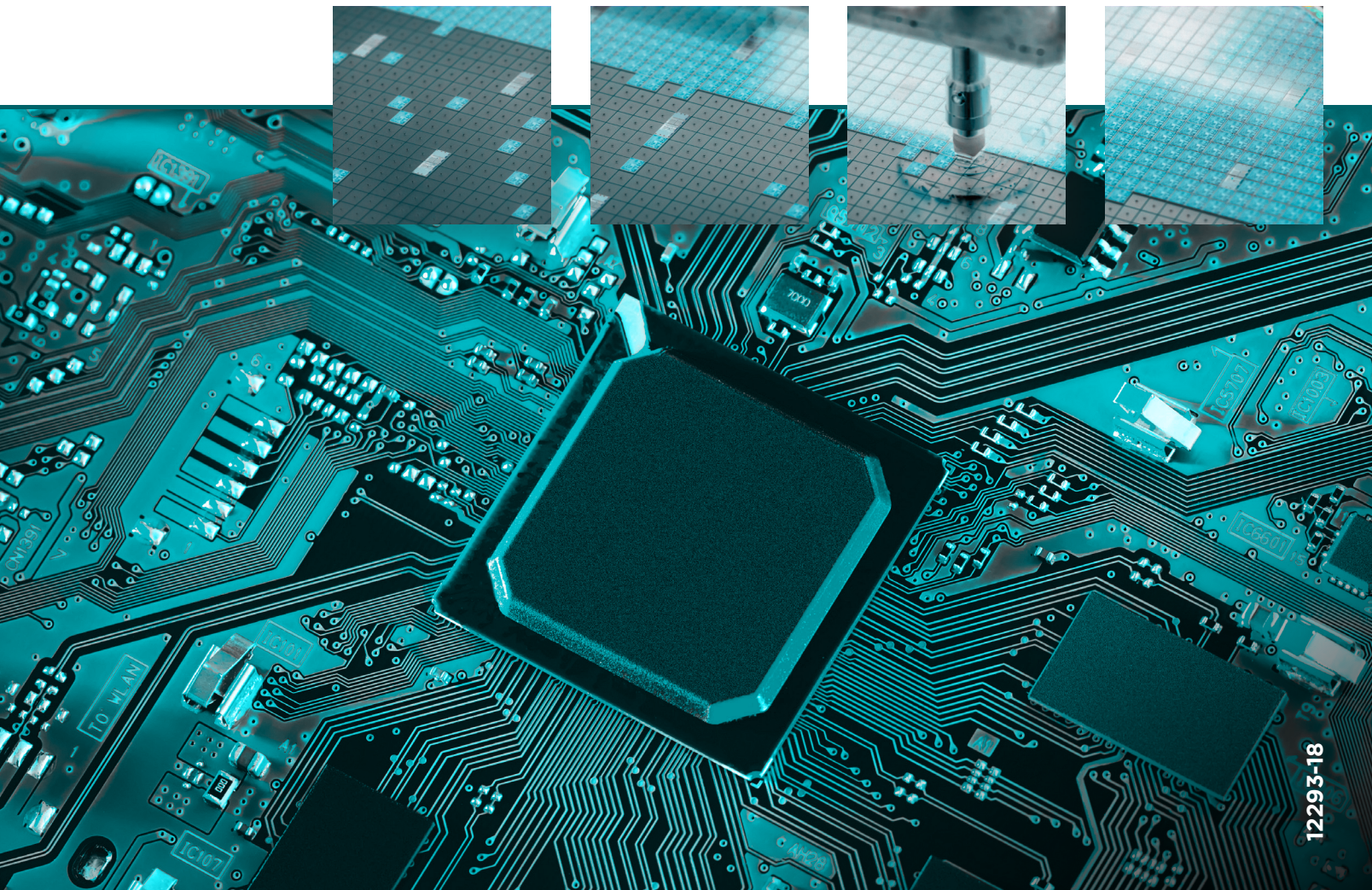
KEY DATES

For a list of meetings
—see page 10

SPIE. **BACUS**

PHOTOMASK TECHNOLOGY GROUP

The Lithography Workshop Makes its Return



The Lithography Workshop Makes its Return

Doug Resnick, *Canon Nanotechnologies Inc.*

During the first week of May, the 27th Lithography Workshop was held at the Sun Valley Resort in Idaho. For those unfamiliar with this event, the Workshop held its first meeting in Lake Placid, New York in 1981. The Workshop is modeled to be similar to a “Gordon-Research” meeting but with the intent of addressing more immediate issues facing the lithography community within the next few years. The attendees of the Workshop share recent advances and knowledge in lithography with others in the community. The Workshop provides an environment where leading researchers from various disciplines can share their thoughts and ideas. The primary intent is to provide an arena for stimulating debate, and the meeting schedule is designed to provide the attendees with time for side-meetings and discussions. Because the networking element is so crucial to the Workshop, the event was postponed twice due to the recent pandemic.

The Workshop has historically focused on leading-edge semiconductor applications but has also addressed the challenging lithography needs of flat panel displays, memory devices, 3-dimensional device integration and advanced packaging. Lately, the Workshop has showcased prominent experts in emerging fields like Quantum Computing and Artificial Intelligence, which are relevant to this audience due to the ubiquitous role lithography plays in the world of computing.

Another unique aspect of the Workshop is the fact that all talks are “invited” talks. The Program Chairs (this year, Andreas Erdmann and I had the honor of putting the program together) select designated topical chairs to recruit speakers. This year, the program consisted of more than sixty talks, six of which were plenary presentations. The program is also presented in a unique way: Sessions during the week are not organized by topic. Instead, the topics (including the plenary talks) are dispersed throughout all of the sessions, creating an environment in which the audience is exposed to all of the immediate issues that are of concern to the lithography community.

This year, the plenary talks were exceptional and featured speakers from industry, the government and academia. The lead plenary presentation was given by Dr. Susan S. Margulies. In her current position, she leads the U.S. National Science Foundation’s Directorate for Engineering and spoke on the importance establishing partnerships with industry and academia. The next plenary was given by Jos Benschop, the Senior Vice President for ASML’s Research, System Engineering and the Technology

Development Center. Jos gave a historical perspective on the development of EUVL and discussed the technology’s roadmap, driven by higher-numerical-aperture systems, along with the required supporting infrastructure. The third plenary was given by Subramanian Iyer, a former IBM fellow who now holds a distinguished professorship position at UCLA. “Subu” emphasized the need to scale bond pad pitches to well under 5 microns as a means for enabling the same benefits that Moore/Denard scaling has accomplished for CMOS chips. Richard Farrell then introduced the potential of Augmented Reality to revolutionize the way people interact and described the need for lithographic processes to enable the fabrication of optical couplers. Alex Liddle is the Chief of the Microsystems and Nanotechnology Division at NIST. Alex gave an engaging and precautionary perspective on the development of lithography back (fondly referred to as the Lithography Wars) in the 1980s and 1990s. The final plenary was given by Nitin Shah, currently a Principal Innovator at Mitre Engenuity. Nitin gave an overview of the US Chips Act and its connection and relevance to other technology programs around the world. Augmented reality and the development of meta optical elements was also a hot topic at the Workshop, as were the papers on advanced packaging.

The relevance and connection to the photomask industry and the conferences designed to support industry were on display the entire week. Just a few examples follow. The development of high-NA EUV lithography requires a mask infrastructure that addresses curvilinear OPC solutions and other co-optimization methods, advanced mask writing, and inspection, and these subjects were covered throughout the Workshop. Emerging device technology has different mask requirements, such as three-dimensional mask structures or slanted relief gratings. This subject matter represents a potential growth area for mask providers. Advanced packaging has its own additional needs, such as masks designed to print fields much larger than the standard 26 mm x 33 mm. The cooperation needed among mask makers, end users, and equipment and software suppliers was also quite apparent.

In summary, the breath and scope of the technology presented was impressive across the four-day event. The next Workshop is scheduled to take place in San Diego, in November of 2024. Please join us, with the purpose of connecting to the community and being part of the conversation. It is worth your time.

FEATURED ARTICLE

In-situ cavitation measurements with a wireless sensor array: applications in megasonic photomask cleaning

Nicolas Candia, *Onda Corp. (United States)*; **Claudio Zanelli**, *Onda Corp. (United States)*; **Zhenxing Han**, *Applied Materials (United States)*; **Petrie Yam**, *Onda Corp. (United States)*

Abstract

Acoustic cavitation continues to be widely used in advanced 193i and EUV megasonic photomask cleaning¹. However, process challenges remain complex as patterns become smaller². Operating within a narrow process window that ensures both full particle removal and pattern damage control is a balancing act that requires many parameters to be optimized and controlled. These include the transducer type, drive frequency, power setting, flow rate, gas concentration, temperature, chemistry, and transducer position^{3, 4, 5, 6, 7}. While batch processing may be more economical for less critical cleaning steps, advanced lithography processes rely on single photomask cleaning technologies because of the increased need for within mask control. Improved cleaning uniformity is achieved through the continuous movement of the photomask and transducer.

In-situ measurement of the acoustic field is required to correlate acoustic parameters with cleaning performance. Previous work introduced a photomask-shaped cavitation sensor array wired to a cavitation meter which characterized how acoustic cavitation varied with parameters such as drive frequency, generator power, transducer distance, and sensor position correlated with cavitation pressure under a static condition⁷. In this study, the technology was extended by developing a wireless sensor array to incorporate the dynamic effects of the photomask rotation and the transducer arm translation. The acoustic pressure uniformity across the photomask was evaluated for varying parameters, including mask rotational speed, transducer arm speed, and exposure time. Pressure measurements of the direct field (PO), stable cavitation (Ps), and transient cavitation (Pt) exhibited distinct signatures that may be indicative of cleaning performance, specifically particle removal or pattern damage.

The high costs of advanced photomask processes have demanded a zero-defect requirement, a constraint prevalent across the semiconductor industry⁸. The study aims to better understand how process variables affect acoustic performance to establish a process control strategy.



BACUS News is published monthly by SPIE for BACUS, the international technical group of SPIE dedicated to the advancement of photomask technology.

Managing Editor/Graphics

Ty Binschus, *SPIE*

Exhibition and Sponsorship Coordinator:

Melissa Valum, *SPIE Sales Representative, Exhibitions and Sponsorships*

BACUS Technical Group Manager

Tim Lamkins, *SPIE*

2023 BACUS Steering Committee

President

Jed Rankin, *IBM Research*

Vice-President

Henry Kamberian, *Photronics, Inc.*

Secretary

Vidya Vaenkatesan, *ASML Netherlands BV*

Newsletter Editor

Artur Balasinski, *Infineon Technologies*

2023 Photomask Technology

Conference Chairs

Ted Liang, *Intel Corp.*

Seong-Sue Kim, *Yonsei University*

Members at Large

Frank E. Abboud, *Intel Corp.*

Uwe F. W. Behringer, *UBC Microelectronics*

Ingo Bork, *Siemens EDA*

Tom Cecil, *Synopsys, Inc.*

Brian Cha, *Entegris Korea*

Aki Fujimura, *D2S, Inc.*

Emily Gallagher, *imec*

Jon Haines, *Micron Technology Inc.*

Koji Ichimura, *Dai Nippon Printing Co., Ltd.*

Bryan Kasprovicz, *HOYA*

Romain J Lallement, *IBM Research*

Khalid Makhmreh, *Applied Materials, Inc.*

Kent Nakagawa, *Toppa Photomasks, Inc.*

Patrick Naulleau, *EUV Tech, Inc.*

Jan Hendrik Peters, *bmbg consult*

Steven Renwick, *Nikon*

Douglas J. Resnick, *Canon Nanotechnologies, Inc.*

Thomas Scheruebl, *Carl Zeiss SMT GmbH*

Ray Shi, *KLA Corp.*

Thomas Struck, *Infineon Technologies AG*

Anthony Vacca, *Automated Visual Inspection*

Andy Wall, *HOYA*

Michael Watt, *Shin-Etsu MicroSi Inc.*

Larry Zurbrick, *Keysight Technologies, Inc.*

SPIE.

P.O. Box 10, Bellingham, WA 98227-0010 USA

Tel: +1 360 676 3290

Fax: +1 360 647 1445

SPIE.org

help@spie.org

©2023

All rights reserved.

FEATURED ARTICLE

Introduction

A common photomask cleaning method relies on particle removal by the application of acoustic streaming and cavitation during wet clean process under acoustic exposure from a megasonic transducer. Acoustic streaming refers to the liquid motion due to viscous attenuation of the sound wave. Acoustic cavitation can be understood through two general effects, stable and transient cavitation. During stable cavitation, bubbles are generated by rapid changes in the direct field pressure, which oscillate in size and dimension associated to harmonic resonance frequencies. The oscillating bubbles create localized microstreaming effects which result in a mechanical pressure from stable cavitation (P_s). When the pressure exceeds a threshold, the bubbles collapse and create localized shockwaves resulting in high levels of transient cavitation pressure (P_t). For precision megasonic cleaning applications for parts such as photomasks, it is commonly understood that stable cavitation predominantly cleans, while transient cavitation contributes to both cleaning and pattern damage. Preserving this process window requires control over the acoustic output to ensure full particle removal while minimizing damage.

An established method to quantify the stable and transient cavitation level is to analyze the acoustic emissions with a hydrophone spectrally. A sample pressure spectrum can be seen below. The primary peak colored in blue represents the direct field frequency (F_0) and pressure (P_0), and the yellow peaks represent the stable cavitation pressure (P_s). The red-colored region represents the signal from the bubble collapse or transient cavitation pressure (P_t)⁹. Uniquely quantifying both P_s and P_t is integral to controlling and monitoring an ultrasonic cleaning process.

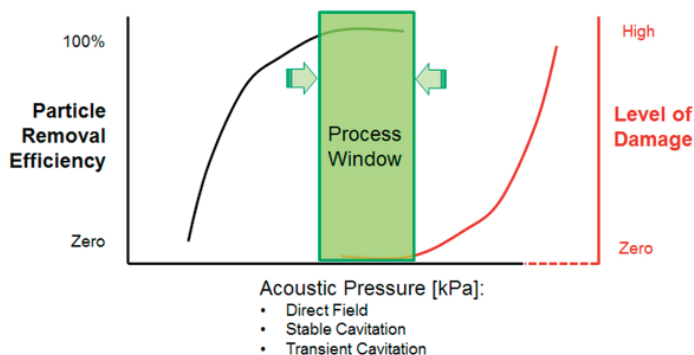


Figure 1. Process window becomes tighter with shrinking feature dimensions and zero-defects requirement.

Materials and Methods

A novel wireless mask sensor array was developed to quantify the acoustic pressure at the surface of a photomask. An array of 3 piezo-electric sensors was integrated into a quartz photomask (152 x 152 x 6 [mm]), each separated by 38 mm across the mask (center, top, and top left). Each sensor was acoustically calibrated based on the Stepped Single frequency comparison technique¹⁰ to measure the output level in physical pressure units [kPa]. The mask sensor array interfaced with a cavitation meter (Onda MCT-2000¹¹) with an electronic bandwidth of 10 MHz that acquired the acoustic pressure spectrum to determine the acoustic pressure from the direct field (P_0), stable cavitation (P_s), transient cavitation (P_t), and the total pressure (P_{tot}).

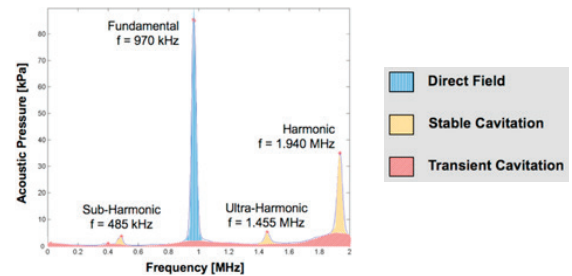


Figure 2. Schematic of acoustic pressure spectrum. The blue area represents the direct field pressure (P_0) generated by the drive frequency (F_0). The yellow areas represent harmonics, sub-harmonic, and ultra-harmonics associated with stable acoustic cavitation pressure (P_s). The red area represents the broadband noise generated from the collapse of bubbles or transient cavitation pressure (P_t).

The wireless mask sensor was placed on a rotational mask chuck while a moving arm with a nozzle transducer swept across the mask sensor.

All experiments were done in de-ionized water at a flow rate of 2.0 [L/min]. The room temperature was 25.4 [°C], and the water was 23.1 [°C]. The dissolved oxygen concentration was 8.6 [mg/L]. The distance between the nozzle and the mask surface was 10 [mm]. The acoustic energy was delivered by a Kaijo Slim Line megasonic generator driving a single nozzle 1 [MHz] transducer.

In this study, data was acquired by the primary sensor located at the center of the wireless sensor. The total acoustic pressure was then logged over time as the mask sensor rotated and the transducer arm swept to create a signature 1D pressure profile. A fixed set of mechanical parameters such as the mask rotation

FEATURED ARTICLE

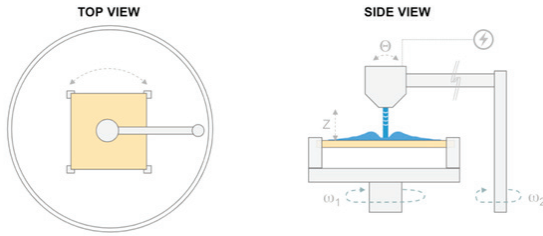


Figure 3. The schematic of a wireless sensor array enables in-situ acoustic cavitation measurements to capture the dynamic effects of the mask rotation and transducer arm sweep.

speed, the transducer sweep speed, and mask size were then applied to a simulation that extrapolated the pressure uniformity relying on the 1D distribution profile that was integrated over time and space. The result of this projected method is a 2D cumulative pressure uniformity map. The method was verified in different ways including reference checks with auxiliary sensors located at the edge of the mask sensor. Furthermore, a proxy sensor mounted at the side of the chamber enabled measurements to check the stability of the acoustic output from the transducer. Finally, the measured 1D profile was checked against simulations that indicated good correlation. Ultimately, cleaning trials were carried out to evaluate the correlation between the cumulative pressure map and erosion patterns.

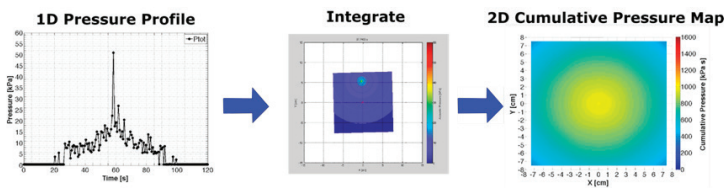


Figure 4. Description of the “projection” method which includes: logging of pressure as transducer sweeps over the primary sensor; extrapolating 1D pressure distribution across the mask surface over the exposure time; determination of the 2D cumulative pressure uniformity with units in [kPa-s].

Using this method, the 2D cumulative pressure distribution was determined under conditions that included varying the electric power (24 and 40 [W]) and the exposure time (240 and 360 [s]). During these studies, the mask rotation speed and transducer arm speed was fixed at 60 [RPM] and 3.86 [mm/s] respectively.

After establishing a reliable method to generate cumulative pressure plots of the total pressure, spectral analysis of each data point was applied. This allowed

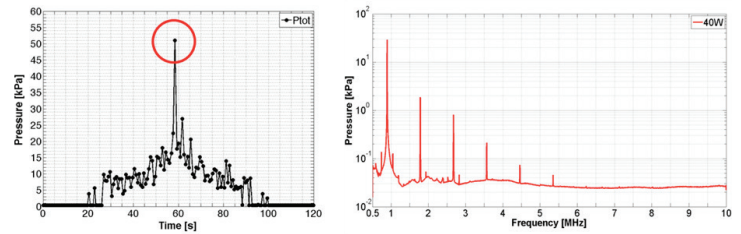


Figure 5. Spectral analysis of each data point enables determination of the pressure from the direct field, stable cavitation, and transient cavitation (P_0 , P_s , P_t).

2D cumulative pressure plots of the total pressure to be separated into plots of the lower level pressure from the direct field, stable cavitation pressure, and transient cavitation by applying the same extrapolation approach.

Results and Discussion

The motivation to develop a wireless sensor array was to account for acoustic influences from additional fluid dynamic effects from the mask rotation and transducer movement. To quantify this, measurements at the primary sensor were compared between static and dynamic conditions. Static conditions imply the mask sensor was stationary as the transducer was aligned with the primary sensor. Dynamic conditions refer to addition of the mask rotation and transducer movement. It was verified that power scales linearly with pressure squared. However, the static and dynamic conditions trend at a different rate, presumably due to fluid dynamic effects. At higher power levels, the total pressure under static and dynamic conditions begins to converge.

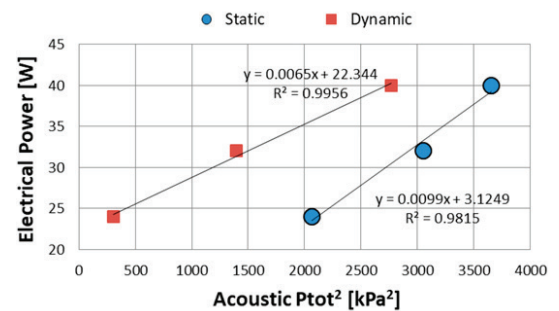


Figure 6. Correlation studies between electrical power and total pressure squared under both static and dynamic conditions. Static conditions include: 1 [MHz], 2.0 [L/min], 24, 32, and 40 [W], location aligned with the primary sensor. Dynamic conditions include the static conditions and also: transducer arm speed 3.86 [mm/s], mask rotation 60 [RPM].

FEATURED ARTICLE

The shape of the 1D pressure profile represents the pressure distribution as the mask rotates and the transducer arm sweeps across the center of the photomask back and forth. This shape is unique to the process conditions and will vary with changing parameters. The 1D profiles shown in Figure 6 were acquired under conditions that include a mask sensor rotational speed of 60 [RPM] and transducer arm speed at 3.86 [mm/s]. The set of 1D profiles represent the nozzle passing over the primary sensor twice, once from the outbound movement and the second from the return of the nozzle, returning back to the original point after 240 [s]. The measured pressure increases as the nozzle approaches the primary sensor at the center, and the pressure decreases as it moves away. When the nozzle moves off the photomask, there is negligible pressure measured. This can be seen in the regions at $t = 30$ and 90 [s] for the first pass and $t = 140$ and 210 [s] on the return pass. This sequence was repeated at two power levels, 24 and 40 [W].

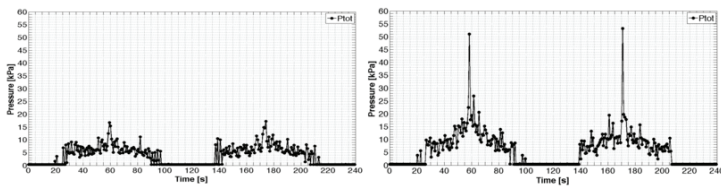


Figure 7. Time evolution of the total pressure obtained by the primary sensor for an arm speed of 3.86 [mm/s] and 60 [RPM] at 24 [W] (left) and 40 [W] (right).

With the 1D profile, 2D cumulative pressure maps were generated by integrating over time and space. Two parameters were compared: (1) generator power and (2) exposure time. In all cases, the cumulative pressure near the center is highest since the linear velocity of the mask sensor is much lower in the center than the edge. However, non-linear effects were observed, likely due to fluid dynamics effects on the changing cavitation behavior at higher power. The ratio of the cumulative pressure at the center is 1.6X, while the edge is 1.4X. When comparing only the exposure time at fixed power levels, the cumulative pressure at the center and edge scale proportionally. Because various process parameters can affect the acoustic pressure, certain conditions may yield similar cumulative pressure maps. For instance, the cumulative pressure was comparable under two conditions: 24 [W] power over 360 [s] of exposure time and 40 [W] power over 240 [s] of exposure time. Some non-linearity effects were observed near the center, likely influenced by the difference in generator power.

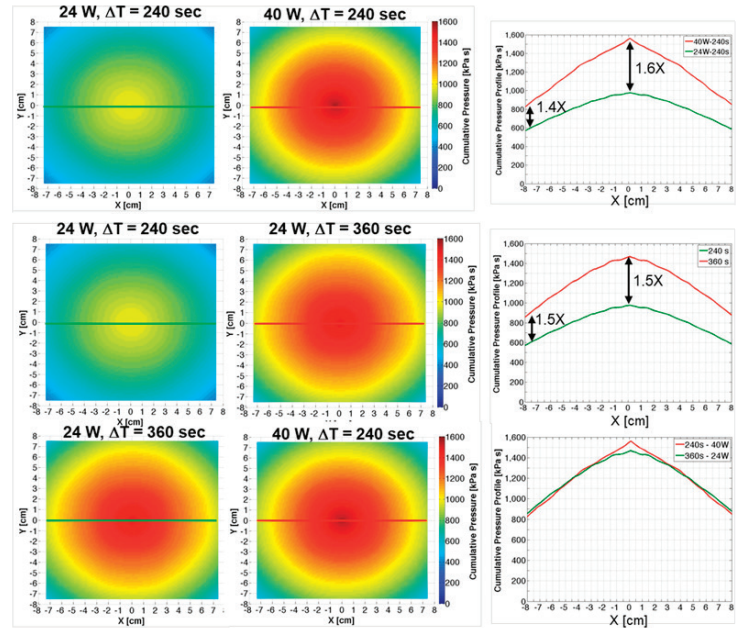


Figure 8. Comparison of the 2D Cumulative pressure for 24 (left) and 40 [W] (middle) at 240 [s] and the cumulative pressure profile through the center of the mask (right). A non-linear effect with the power can be observed.

Ultimately, the correlation to cleaning performance is most essential. Coupons were prepared with a blue ink painted onto an Aluminum 150x150 [mm] plate. The coupons were then placed on the mask chuck and were exposed to the same process conditions as the mask sensor, namely at an arm speed of 3.86 [mm/s], rotation speed of 60 [RPM], power levels of 24 [W] and 40 [W], and exposure time of 240 [s] and 360 [s].

Unlike the cumulative pressure plots, the erosion patterns trended differently with increasing power and time. At 24 [W] and 240 [s] and even 360 [s] of exposure time, the erosion pattern was negligible. However, at 40 [W], the erosion pattern was clear after 240 [s] of exposure and more evident after 360 [s]. A threshold between 24 [W] and 40 [W] is seemingly

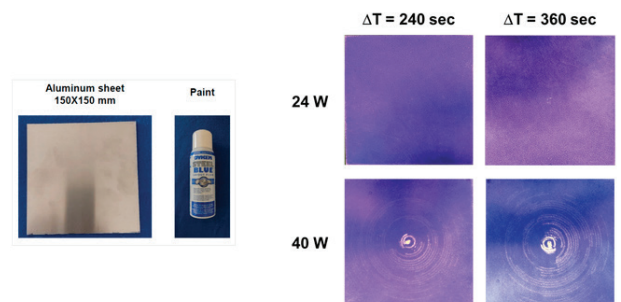


Figure 9. Erosion patterns for power levels at 24 and 40 [W] and exposure times of 240 and 360 [s] indicate the presence of a pressure threshold where cleaning starts to take effect.

FEATURED ARTICLE

present. The erosion of the paint takes place only after exceeding this threshold. This insight may be useful when developing a mask cleaning process that requires optimizing parameters that affect fluid dynamic and acoustic cavitation effects.

To further investigate, 2D cumulative pressure plots were generated for the acoustic pressure from the direct field, stable cavitation, and transient cavitation (PO, Ps, and Pt). Similar bullseye patterns are observed for all three components, but it is evident the transient cavitation pressure (Pt) is relatively lower. Also, the distribution of transient cavitation is localized to the area directly below the nozzle, whereas Ps and Pt exhibit a wider distribution. The previous study with a wired mask sensor array also concluded this⁷.

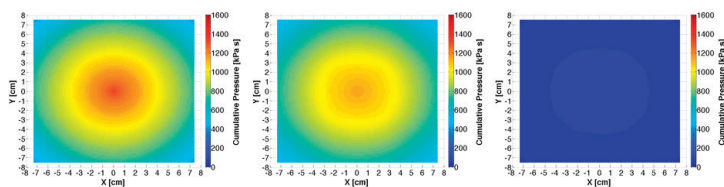


Figure 10. Cumulative pressure for PO, Ps, and Pt for 40W at 240s.

Conclusions

A complete acoustic measurement solution was presented which relied on several components: a wireless mask sensor array for in-situ measurements, a reference sensor that checks the acoustic stability and accuracy of the transducer, a “projection method” that is based on extrapolating the 1D pressure distribution across the mask surface over time, and spectral analysis of the detected acoustic emissions to quantify the pressure from the direct field, stable cavitation, and transient cavitation. The combination provides a means to make in-situ acoustic measurements in a complex and dynamic cleaning process. Through experimentation and modeling, various process parameters can be characterized to determine how each correlates with the acoustic performance. Future work must include correlation studies with particle removal and damage.

REFERENCES



- 1 M. Keswani, R. Balachandran, and P. Deymier, "Megasonic Cleaning for Particle Removal", in: Particle Adhesion and Removal, K. L. Mittal and R. Jaiswal (Eds.), Ch. 6, pp. 243-279, Wiley-Scrivener Publishing, Beverly, MA (2015).
- 2 The International Technology Roadmap for Semiconductors (ITRS) for Lithography 2013 Edition, Tables LITH3 and LITH4, Semiconductor Industry Association, Washington, DC (2013).
- 3 S. Helbig, S. Urban, E. Klein, and S. Singh, "Impact of Megasonic Process Conditions on PRE and Sub-Resolution Assist Feature Damage", in: Photomask Technology 2008, H. Kawahira and L. S. Zurbrick (Eds.), Proc. SPIE 7122, p. 712210 (2008).
- 4 G. W. Gale and A. A. Busnaina, "Roles of Cavitation and Acoustic Streaming in Megasonic Cleaning", Particulate Sci. Technol. 17, 229 (1999).
- 5 W. Kim, T. H. Kim, J. Choi, and H. Y. Kim, "Mechanism of Particle Removal by Megasonic Waves", Appl. Phys. Lett. 94, 081908 (2009).
- 6 B. K. Kang, M. S. Kim, and J. G. Park, "Effect of Dissolved Gases in Water on Acoustic Cavitation and Bubble Growth Rate in 0.83 MHz Megasonic of Interest to Wafer Cleaning", Ultrason. Sonochem. 21, 1496 (2014).
- 7 N. Candia, C. Zanelli, J. Brunner, J. Straka, Z. Han, S. Howard, P. Yam, "Characterization of Acoustic Cavitation from a Megasonic nozzle transducer for Photomask Cleaning", Proc. SPIE 10451, p. 1045114 (2017). doi:10.1117/12.2281275.
- 8 B. J. Grenon, K. Bhattacharyya, and B. Eynon, "A New Generation of Progressive Mask Defects on the Pattern Side of Advanced Photomasks", 22nd European Mask and Lithography Conference, Proc. SPIE 6281, p. 62810J (2006).
- 9 J. Frohly, S. Labouret, C. Bruneel, I. Looten-Baquet, R. Torguet, "Ultrasonic cavitation monitoring by acoustic noise power measurement", J. Acoust. Soc. Am. 108 (5), 2012-2020 (2000)
- 10 A. Selfridge and P.A. Lewin, "Wideband Spherically Focused PVDF Acoustic Source for Calibration of Ultrasound Hydrophone Probes", IEEE Trans. UFFC 47(6) 1372-1376 (2000).
- 11 ondasonics.com/wp-content/uploads/2017/09/Onda_HCT-0320_MCT-2000_DataSheet.pdf

INDUSTRY BRIEFS

Reflections on Photomask Japan 2023 (PMJ2023): embracing the era of curvilinear masks by Seiji Nagahara, TEL

One session that particularly stood out during PMJ2023 was the Panel Discussion on curvilinear masks. Moderated by Kokoro Kato-san (PMJ2023 Steering Committee Chair, Synopsys, Inc.) and Hiroshi Nakata-san (PMJ2023 Program Committee Vice Chair, Dai Nippon Printing Co., Ltd. (DNP), the panel delved into various aspects of curvilinear masks. Kato-san initiated the discussion by emphasizing the need for the entire mask industry to prepare for the new ecosystem surrounding curvilinear data handling, manufacturing, and inspection/metrology. He shared insights from the eBeam Initiative Survey, revealing that 76% of respondents expressed confidence and optimism regarding the utilization of curvilinear masks.

semiengineering.com/reflections-on-photomask-japan-2023-embracing-the-era-of-curvilinear-masks/?cmid=07ec6642-5d65-406a-bdec-2a9377c1c23b

Mycronic receives order for an SLX mask writer

BACUS News Editorial Note:

This is the 40th SLX machine in their press releases going back to their first SLX order press release in January 2020

STOCKHOLM, April 25, 2023 /PRNewswire/ Mycronic AB (publ) has received an order for an SLX mask writer from a new customer in Asia. The order value is in the range of USD 7-9 million. Delivery of the system is planned for the fourth quarter of 2023.

[Mycronic receives order for an SLX mask writer \(prnewswire.co.uk\)](https://prnewswire.co.uk)

Nanoimprint finally finds its footing

Nanoimprint lithography, which for decades has trailed behind traditional optical lithography, is emerging as the technology of choice for the rapidly growing photonics and biotech chips markets. First introduced in the mid-1990s, nanoimprint lithography (NIL) has consistently been touted as a lower-cost alternative to traditional optical lithography. Even today, NIL potentially is capable of matching current EUV dimensions, yield, and throughput using fewer process steps and significantly lower capital equipment costs.

[Nanoimprint Finally Finds Its Footing \(semiengineering.com\)](https://semiengineering.com)

Rapidus gets another \$2bn

BACUS News Editorial Note:

Rapidus is the first EUV fab in Japan, bringing the worldwide production fab total to six.

The Japanese government will provide Rapidus with an additional \$1.94 billion to add to the \$2.5 billion it has already received, reports the Nikkei. The total project to get 2nm chips into volume production will cost \$37 billion. Rapidus aims to begin mass production of 2nm ICs in the late 2020s. It took a technology licence from IBM in 2022 which had produced a 2nm prototype in 2021.

electronicsweekly.com/news/business/819237-2023-04/

EUV Tech introduces new multi-use actinic EUV metrology tool

MARTINEZ, CALIFORNIA, UNITED STATES, May 11, 2023/EINPresswire.com/

EUV Tech, a global leader in the production of at-wavelength EUV metrology tools, is excited to announce the release of the new EUV N&K and Phase Measurement Tool, its latest innovation in extreme ultraviolet lithography (EUVL) technology. The multi-use EUV N&K and Phase Measurement Tool is designed for direct actinic measurement of the optical properties of materials in the Extreme Ultraviolet (EUV) regime.

[EUV Tech Introduces New Multi-Use Actinic EUV Metrology Tool | Today in Science](https://www.euv-tech.com/news/euv-tech-introduces-new-multi-use-actinic-euv-metrology-tool-today-in-science)

NVIDIA boss pitches generative AI for chip manufacturing

Chip manufacturing is an “ideal application” for GPUs running generative AI algorithms says Jensen Huang, CEO of Nvidia. Speaking at imec’s ITF World 2023 semiconductor conference in Antwerp, Belgium, by video, Huang points to customers such as KLA, Applied Materials and Hitachi.

europeanew.com/en/nvidia-boss-pitches-generative-ai-for-chipmanufacturing/

MEMBERSHIP

Join the premier professional organization for mask makers and mask users

About the BACUS Group

Founded in 1980 by a group of chrome blank users wanting a single voice to interact with suppliers, BACUS has grown to become the largest and most widely known forum for the exchange of technical information of interest to photomask and reticle makers. BACUS joined SPIE in January of 1991 to expand the exchange of information with mask makers around the world.

The group sponsors an informative monthly meeting and newsletter, BACUS News. The BACUS annual Photomask Technology Symposium covers photomask technology, photomask processes, lithography, materials and resists, phase shift masks, inspection and repair, metrology, and quality and manufacturing management.

Individual Membership benefits include:

- Subscription to BACUS News (monthly)
- Eligibility to hold office on BACUS Steering Committee

Corporate Membership benefits include:

- 3-10 Voting Members in the SPIE General Membership, depending on tier level
- Subscription to BACUS News (monthly)
- One online SPIE journal subscription
- Listed as a Corporate Member in the BACUS News

spie.org/bacushome

Key Dates

2023

European Mask and Lithography Conference (EMLC)

19-21 June 2023

Dresden, Germany

emlc-conference.com

SPIE Photomask Technology + EUV Lithography

1-5 October 2023

Monterey, California, USA

spie.org/puv

2024

SPIE Advanced Lithography + Patterning

25-29 February 2024

San Jose, California, USA

spie.org/al

Photomask Japan

16-18 April 2024

Yokohama Japan

smartconf.jp

You are invited to submit events of interest for this calendar. Please send to tyb@spie.org.



Sponsorship Opportunities

Sign up now for the best sponsorship opportunities

Photomask Technology +
EUV Lithography 2023

Contact:

Melissa Valum, Tel: +1 360 685 5596

Advanced Lithography +
Patterning 2023

Contact:

Melissa Valum, Tel: +1 360 685 5445
melissav@spie.org

Kim Abair, Tel: +1 360 685 5499
kima@spie.org

Advertise in the BACUS News

The BACUS newsletter is the premier publication serving the photomask industry. For information on how to advertise, contact:

Melissa Valum, Tel: +1 360 685 5596
melissav@spie.org

BACUS Corporate Members

Acuphase Inc.
American Coating Technologies LLC
AMETEK Precitech, Inc.
Berliner Glas KGaA Herbert Kubatz GmbH & Co.
FUJIFILM Electronic Materials U.S.A., Inc.
Gudeng Precision Industrial Co., Ltd.
Halocarbon Products
HamaTech APE GmbH & Co. KG
Hitachi High Technologies America, Inc.
JEOL USA Inc.
Mentor Graphics Corp.
Molecular Imprints, Inc.
Panavision Federal Systems, LLC
Profilcolore Srl
Raytheon ELCAN Optical Technologies
XYALIS

SPIE.

P.O. Box 10, Bellingham, WA 98227-0010 USA

Tel: +1 360 676 3290

SPIE.org

help@spie.org

©2023

Shipping Address

1000 20th St.,
Bellingham, WA 98225-6705 USA